PHYSICAL REVIEW B VOLUME 46, NUMBER 13 1 OCTOBER 1992-I

Superconducting and magnetic properties of the heavy-fermion compounds UT_2Al_3 (T=Ni,Pd)

Y. Dalichaouch, M. C. de Andrade, and M. B. Maple
Department of Physics and Institute for Pure and Applied Physical Sciences, University of California, San Diego, La Jolla, California 92093
(Received 22 May 1992)

The resistive upper critical field H_{c2} as a function of temperature T has been determined for polycrystalline specimens of the isostructural antiferromagnetic heavy-fermion superconductors UT_2Al_3 (T=Ni, Pd). The zero-temperature superconducting coherence lengths ξ_0=190 Å (77 Å) for T=Ni (Pd) have been estimated from the initial slope of $H_{c2}(T)$, and analyses of previously reported specific-heat data yield an effective mass enhancement $m^*/m_e \sim 40$ (49) for T=Ni (Pd), where m_e is the free-electron mass. High-precision measurements of the normal-state electrical resistivity reveal a broad anomaly below 4.6 K in UNi_2Al_3, which correlates with the onset of U-moment antiferromagnetic ordering. In UPd_2Al_3, the large electrical resistivity drop between T_c and $T_N \approx 15$ K can be accurately described by an expression that is appropriate for an antiferromagnet with an energy gap $\Delta \approx 40$ K and an additional T^2 term reflecting Fermi-liquid behavior.

Perhaps the most significant recent developments in heavy-fermion (HF) superconductors have been the discovery of antiferromagnetic (AFM) ordering with very small U moments ($0.01\mu_B$-$0.1\mu_B$) in compounds previously thought to be nonmagnetic and the delineation of complex and multicomponent superconducting phase diagrams.[1] In all cases, except perhaps UBe_{13}, superconductivity coexists with AFM ordering at low temperatures, and it is believed that the interaction between the superconducting and magnetic order parameters can lead to additional symmetry breakdown and further transitions inside the superconducting state in unconventional superconductors.

Heavy-fermion superconductivity has recently been reported in two new U-based compounds: UNi_2Al_3 (Ref. 2) and UPd_2Al_3 (Ref. 3), which exhibit AFM transitions at T_N=4.6 K and T_N=14 K followed by transitions to superconducting states at $T_c \approx 1$ K and $T_c \approx 2$ K, respectively. According to neutron-scattering experiments,[4] the ordered magnetic moment in UPd_2Al_3 lies in the basal plane and is about $(0.85\pm0.03)\mu_B$/U atom, whereas no long-range magnetic order could be detected above 1.5 K in UNi_2Al_3. However, zero-field muon spin-relaxation experiments revealed a commensurate AF structure in the latter compound[5] in which the U moments, assumed to be along the c axis, are of the order of $0.1\mu_B$/U atom and a much smaller ordered moment ~ 0.01-$0.1\mu_B$/U atom in UPd_2Al_3.[6] The normal-state electrical resistivity $\rho(T)$ of UNi_2Al_3 is reminiscent of that of UPt_3 in that ρ increases monotonically with increasing temperature and has substantial negative curvature.[7] On the other hand, the $\rho(T)$ curve of UPd_2Al_3 resembles that of URu_2Si_2 with ρ first increasing with increasing temperature, passing through a maximum around 80 K, and decreasing with further increase in T.[8] While specific heat and magnetic susceptibility measurements were reported to exhibit anomalies at T_N in both compounds, the $\rho(T)$ data showed a kink only in UPd_2Al_3, and no feature was observed in UNi_2Al_3.[2,3] In this paper, we report resistive measurements of the upper critical field H_{c2} as a function of temperature and high-precision measurements of the low-temperature normal-state resistivity with particular attention on the antiferromagnetic transitions in UT_2Al_3 (T=Ni and Pd) compounds.

The polycrystalline specimens of UT_2Al_3 (T=Ni,Pd) were prepared by arc melting in an argon atmosphere and were then vacuum annealed for either 8 days at 900 °C (T=Pd) or 12 days at 1000 °C (T=Ni). X-ray diffraction patterns were indexed to the hexagonal $PrNi_2Al_3$-type crystal structure with the space group $P6/mmm$ and lattice parameters a=5.217 Å and c=4.024 Å for UNi_2Al_3 and a=5.419 Å and c=4.052 Å for UPd_2Al_3. The electrical resistivity was measured in a ^{3}He-^{4}He dilution refrigerator using an LR 201 four-lead ac nanoohmmeter operating at 16 Hz and a measuring current density of ~ 8 mA/cm^2. The applied magnetic field was produced using a superconducting solenoid, and the superconducting critical temperature T_c was defined as the temperature at which the resistivity decreases to 50% of its extrapolated normal-state value.

Zero-field electrical resistivity ρ vs temperature T data between 1 and 10 K for UNi_2Al_3 are displayed in Fig. 1. In contrast to the data reported in Ref. 2 in which $\rho(T)$ is linear down to T_c, Fig. 1 reveals a broad shoulder in $\rho(T)$ in the vicinity of T_N followed by a transition to the superconducting state at $T_c \approx 1$ K. The value of $T_N \approx 4.6$ K, defined as the temperature corresponding to the minimum in the $d\rho/dT$ vs T curve shown in the inset of Fig. 1, is in excellent agreement with the Néel temperature of the U moments estimated from specific heat and magnetization measurements.[2]

Shown in Fig. 2 are ρ vs T data for UPd_2Al_3 below 25 K. There is an abrupt and large decrease in $\rho(T)$ at $T_N \approx 15$ K due to the onset of U long-range antiferromagnetic order followed by a transition to the superconducting state at $T_c \approx 2$ K. An excellent fit to the data between

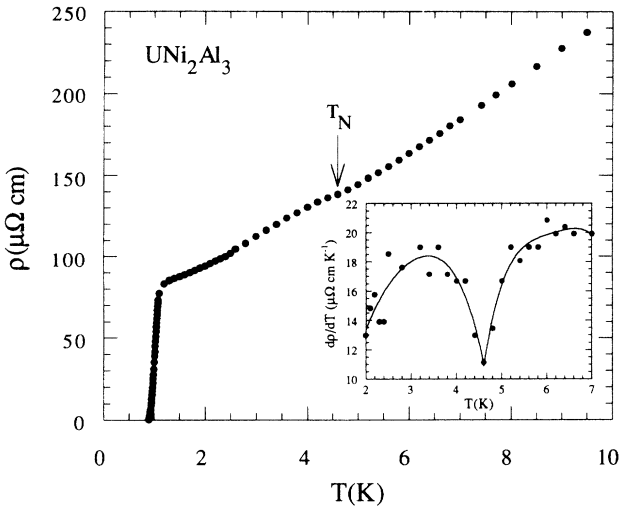

FIG. 1. Low-temperature electrical resistivity ρ vs temperature T of UNi_2Al_3 in zero applied magnetic field. Shown in the inset is the temperature coefficient of resistivity $d\rho/dT$ vs T.

2 and 15 K can be achieved using the sum of an expression appropriate for an antiferromagnet with an energy gap[9] and a T^2 term reflecting Fermi-liquid behavior,

$$\rho=\rho_0+bT[1+2T/\Delta]\exp(-\Delta/T)+cT^2 . \quad (1)$$

The parameters $\rho_0=1$ $\mu\Omega$ cm, $b=24$ mΩ cm/K, $\Delta=40$ K, and $c=0.23$ $\mu\Omega$ cm/K^2 were obtained from the fit. It is interesting to note that even though $\rho(T)$ in URu_2Si_2 is also described by Eq. (1), a narrow peak associated with the spin-density-wave transition develops in the vicinity of $T_N=17.5$ K in URu_2Si_2 but is absent in UPd_2Al_3. The increase of ρ with decreasing T around T_N was first recognized in Cr as being due to the formation of an energy gap on the Fermi surface, which decreases the effective number of carriers.[10] A possible reason for the absence of a peak at T_N in UPd_2Al_3 could be the combined effects of the larger c parameter and the greater fraction of ungapped electron states[11] than in URu_2Si_2. In contrast to UPd_2Al_3, the $\rho(T)$ magnetic anomaly is considerably smaller and smeared out in UNi_2Al_3. A plot of $d\rho/dT$ vs T, shown in the inset of Fig. 1, reveals a T dependence reminiscent of URu_2Si_2 in that ρ first decreases rapidly upon lowering T from above T_N, then less quickly as $T\rightarrow T_N$, and finally decreases rapidly again with decreasing T below T_N. There is a small change in the electronic specific-heat coefficient γ from 150 to 120 mJ/mol K^2 in UNi_2Al_3 as T is cooled through T_N.[2] The reason for the small size of the magnetic anomaly in UNi_2Al_3 is not yet understood. However, it is well known that no feature at all has been seen at $T_N\approx 5$ K in transport and bulk properties of the HF superconductor UPt_3, even though neutron-diffraction measurements show an ordered moment of $(0.02\pm0.01)\mu_B$/U atom.[12]

Representative resistive superconducting transition curves for applied fields up to 32 kOe are displayed in Figs. 3(a) and 4(a) for UNi_2Al_3 and UPd_2Al_3, respectively. The ρ value of the UPd_2Al_3 sample used for these measurements is one order of magnitude larger than that of the piece used for the normal-state resistivity, even

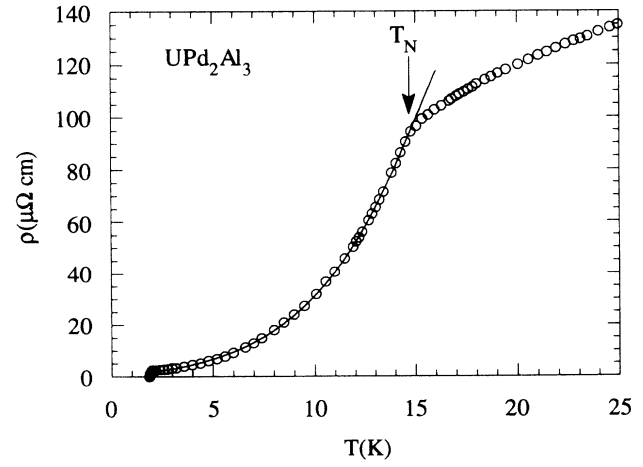

FIG. 2. Low-temperature electrical resistivity vs temperature T of UPd_2Al_3 in zero applied magnetic field. The solid line represents a fit of the equation $\rho=\rho_0+bT[1+2T/\Delta]\exp(-\Delta/T)+cT^2$ to the data with parameters ρ_0, b, Δ, and c that are given in the text.

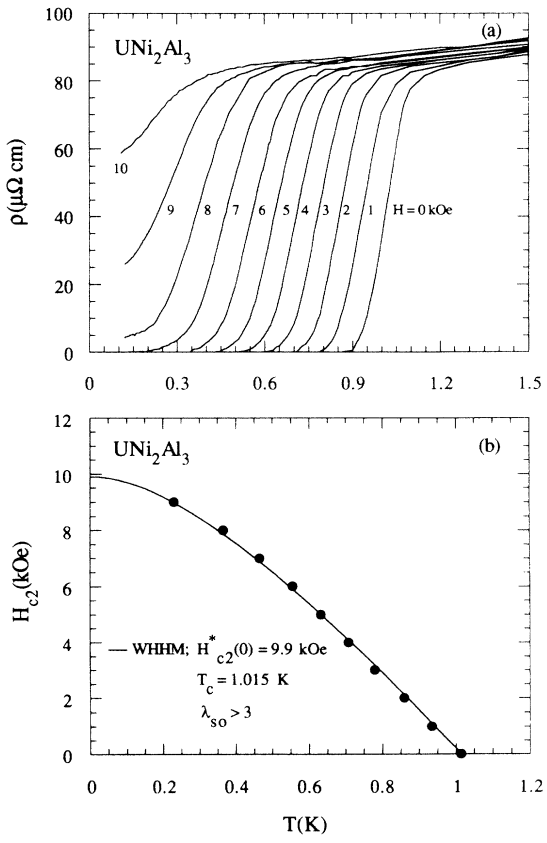

FIG. 3. (a) Resistive superconducting transition curves for UNi_2Al_3 in various applied magnetic fields up to 10 kOe and (b) upper critical field H_{c2} vs temperature T determined from $\rho(T,H)$ data for UNi_2Al_3. The solid line is a fit to the data that was calculated from the WHHM theory assuming only orbital pair breaking. The spin-orbit scattering parameter λ_{so} consistent with this absence of paramagnetic limitation is also shown in the figure.

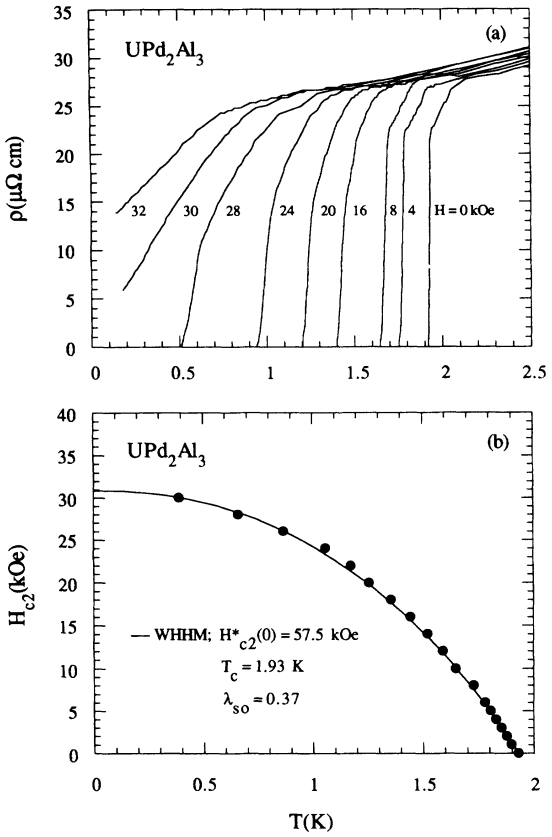

FIG. 4. (a) Resistive superconducting transition curves for UPd_2Al_3 in various applied magnetic fields up to 32 kOe (for clarity, data for some fields are not shown) and (b) upper critical field H_{c2} vs temperature T determined from $\rho(T,H)$ data for UPd_2Al_3. The solid line is a fit to the data that was calculated from the WHHM theory with parameters shown in the figure.

though both pieces were cut from the same ingot. This discrepancy is likely due to macroscopic cracks present in the sample, which can be seen under the microscope. The upper critical field $H_{c2}(T)$ curves extracted from the $\rho(T,H)$ data are shown in Figs. 3(b) and 4(b).

The initial slopes of the H_{c2} vs T curves have the values $(-dH_{c2}/dT)_{T_c}=13$ kOe/K for $T=$Ni and 43 kOe/K for $T=$Pd, which can be used to estimate ξ_0, the superconducting coherence length at $T=0$ K. The zero-temperature orbital critical magnetic field $H_{c2}^*(0)$ can be determined from the weak-coupling formula[13]

$$H_{c2}^*(0)=0.693[(-dH_{c2}/dT)_{T_c}]T_c \ , \tag{2}$$

which gives $H_{c2}^*(0)\sim 9.1$ kOe for UNi_2Al_3 ($T_c=1.02$ K) and ~ 57.5 kOe for UPd_2Al_3 ($T_c=1.93$ K). These values can then be used to calculate the Ginzburg-Landau coherence lengths using the following expression:

$$H_{c2}^*(0)=\frac{\Phi_0}{2\pi\xi_0^2} \ , \tag{3}$$

where $\Phi_0=hc/2e=2.07\times10^{-7}$ Oe cm^2 is the flux quantum. The calculations give $\xi_0=190$ Å for $T=$Ni and $\xi_0=77$ Å for $T=$Pd.

The paramagnetic limiting field at $T=0$ K, H_{p0}, in the absence of spin-orbit scattering, is given by

$$H_{p0}(0)=18.4T_c \ \text{(kOe)} \tag{4}$$

which yields $H_{p0}=18.7$ kOe for $T=$Ni and $H_{p0}=35.5$ kOe for $T=$Pd. It is interesting to note that $H_{c2}(0)\approx H_{c2}^*(0)$ for UNi_2Al_3, whereas $H_{c2}(0)\approx H_{p0}$ for UPd_2Al_3.

The coherence length can also be obtained from the BCS equation[14]

$$\xi_0=0.18\frac{\hbar v_F}{k_B T_c} \ . \tag{5}$$

However, it is necessary to estimate the Fermi velocity $v_F=\hbar k_F/m^*$, where k_F is the Fermi wave vector. Assuming a spherical Fermi surface, $k_F=(3\pi^2Z/\Omega)^{1/3}$, where Z is the number of conduction electrons per unit cell and Ω is the unit-cell volume. As a rough approximation, we assume that there are three $5f$ electrons contributed by each U atom so that $Z=3$, since there is one formula unit per unit cell. From the hexagonal lattice parameters determined from x-ray measurements, we find $\Omega=9.5\times10^{-23}$ cm^3 for UNi_2Al_3 and $\Omega=10.29\times10^{-23}$ cm^3 for UPd_2Al_3. We then obtain $k_F=9.78\times10^7$ cm^{-1} and 9.52×10^7 cm^{-1}, respectively. The effective mass can be deduced from the relation

$$m^*=\frac{\hbar^2k_F^2\gamma}{\pi^2(Z/\Omega)k_B^2} \ , \tag{6}$$

which gives $m^*=41m_e$ for $T=$Ni and $m^*=49m_e$ for $T=$Pd, using the previously reported electronic specific-heat γ values for different samples.[2,3] Equation (5) then yields the values $\xi_0=371$ Å for UNi_2Al_3 and $\xi_0=160$ Å for UPd_2Al_3, which are in reasonable agreement with the values inferred from H_{c2}, considering the approximations that were made.

The Werthamer, Helfand, Hohenberg, and Maki (WHHM) theory[15] for the calculation of $H_{c2}(T)$ provides a good fit to the experimental data of both UNi_2Al_3 and UPd_2Al_3, as shown in Figs. 3(b) and 4(b). Paramagnetic limitation does not play any role in UNi_2Al_3 so that $H_{c2}(T)$ is completely determined by orbital effects. The absence of paramagnetic limitation is also consistent with an equal-spin pairing superconducting state (p wave) as was suggested for UPt_3.[16] The $H_{c2}^*(0)=9.9$ kOe value used in the fit is slightly higher than the value calculated from Eq. (2), an effect which can be due to anisotropic or multiband effects. On the other hand, the $H_{c2}(T)$ curve for UPd_2Al_3 shows an appreciable flattening at low temperatures, similar to $CeCu_2Si_2$,[17] which indicates strong spin pair-breaking effects as corroborated by the small value of the spin-orbit scattering parameter $\lambda_{so}=0.37$ yielded by the fit. This suggests an even-parity superconducting order parameter or a Balian-Werthamer-type "triplet" spin pairing in UPd_2Al_3.

Analysis of the H_{c2} data reported herein yield estimates for ξ_0 of ~ 190 Å in UNi_2Al_3 and ~ 77 Å in UPd_2Al_3, which are consistent with the respective effective-mass values m^* of $\sim 40m_e$ and $\sim 49m_e$, within the approximations made. The AFM transition at

$T_N = 14$ K in UPd_2Al_3 appears to involve a gap $\Delta \approx 40$ K opening over $\sim 30\%$ of the Fermi surface. The AFM ordering anomaly at $T_N = 4.6$ K in UNi_2Al_3 is smeared out and is less pronounced than in UPd_2Al_3.

The research was supported by the U.S. National Science Foundation under Grant No. DMR 91-07698. M.C.A. gratefully acknowledges support from the CNPq, Brazil.

[1]For a recent review, see M. Sigrist and K. Ueda, Rev. Mod. Phys. **63**, 239 (1991).

[2]C. Giebel, S. Thies, D. Kaczorowski, A. Mehner, A. Grauel, B. Seidel, U. Ahlheim, R. Helfrich, K. Peterson, C.D. Bredl, and F. Steglich, Z. Phys. B **83**, 305 (1991).

[3]C. Geibel, C. Schank, S. Thies, H. Kitazawa, C. D. Bredl, A. Böhm, M. Rau, A. Grauel, R. Caspary, R. Helfrich, U. Ahlheim, G. Weber, and F. Steglich, Z. Phys. B **84**, 1 (1991).

[4]A. Krimmel, P. Fischer, B. Roessli, H. Maletta, C. Geibel, C. Schank, A. Grauel, A. Loidl, and F. Steglich, Z. Phys. B **86**, 161 (1992).

[5]A. Amato, C. Geibel, F. N. Gygax, R. H. Heffner, E. Knetsch, D. E. MacLaughlin, C. Schank, A. Schenk, F. Steglich, and M. Weber, Z. Phys. B **86**, 159 (1992).

[6]Y. J. Uemura (private communication).

[7]G. R. Stewart, Z. Fisk, J. O. Willis, and J. L. Smith, Phys. Rev. Lett. **52**, 679 (1984).

[8]M. B. Maple, J. W. Chen, Y. Dalichaouch, T. Kohara, C. Rossel, M. S. Torikachvili, M. W. McElfresh, and J. D. Thompson, Phys. Rev. Lett. **56**, 185 (1986).

[9]N. H.Andersen, in *Crystalline Electric Field and Structural Effects in f-electron Systems,* edited by J. E. Crow, R. P. Guertin, and T. W. Mihalisin (Plenum, New York, 1980), p. 373.

[10]A. L. Trego and A. R. Mackintosh, Phys. Rev. **166**, 495 (1968).

[11]From the ratio of $\gamma = 210$ mJ/mol K^2 above T_N to the low temperature $\gamma = 150$ mJ/mol K^2 above T_c (Ref. 3), we estimate that the gap opens over $\sim 30\%$ of the Fermi surface in UPd_2Al_3.

[12]G. Aeppli, E. Bucher, C. Broholm, J. Kjems, J. Baumann, and J. Hufnagel, Phys. Rev. Lett. **60**, 615 (1988).

[13]R. R. Hake, Appl. Phys. Lett. **10**, 186 (1967).

[14]See, for example, M. Tinkham, *Introduction to Superconductivity* (McGraw-Hill, New York, 1975).

[15]N. R. Werthamer, E. Helfand, and P. C. Hohenberg, Phys. Rev. **147**, 295 (1966); K. Maki, *ibid.* **148**, 392 (1966).

[16]G. Stewart, Z. Fisk, J. O. Willis, and J. L. Smith, Phys. Rev. Lett. **52**, 679 (1984); F. Steglich, in *Theory of Heavy Fermion and Valence Fluctuations,* edited by T. Kasuya and T. Saso (Springer-Verlag, New York, 1985), p. 23.

[17]F. Steglich, C. D. Bredl, W. Lieke, U. Rauchschwalbe, and G. Sparn, Physica B **126**, 82 (1984).